

## Article

# Synthesis and Application of Modified Lignin Polyurea Binder for Manufacturing a Controlled-Release Potassium Fertilizer

Mingyang Li <sup>1,2</sup>, Gaoyang E <sup>1,2</sup>, Conghui Wang <sup>1,2</sup>, Ruolin Shi <sup>1,2</sup>, Junxi Wang <sup>1,2</sup>, Shuo Wang <sup>1,2</sup>, Yu Wang <sup>3</sup>, Qi Chen <sup>1,2</sup>, Zeli Li <sup>1,2</sup> and Zhiguang Liu <sup>1,2,\*</sup>

<sup>1</sup> National Engineering Research Center for Efficient Utilization of Soil and Fertilizer Resources, College of Resources and Environment, Shandong Agricultural University, Tai'an 271018, China

<sup>2</sup> National Engineering & Technology Research Center for Slow and Controlled Release Fertilizers, College of Resources and Environment, Shandong Agricultural University, Tai'an 271018, China

<sup>3</sup> State Key Laboratory of Soil and Sustainable Agriculture, Institute of Soil Science, Chinese Academy of Sciences, Nanjing 210008, China

\* Correspondence: zhiguang1987@sdau.edu.cn

**Abstract:** Conventional potassium chloride granules have inefficient applications in agricultural production due to particle irregularity and low fluidity. The application of controlled-release potassium chloride could increase the potassium-use efficiency and alleviate the shortage of potassium ore resources. In this study, a well-rounded potassium chloride fertilizer core was prepared, using the graft modification of polyurea to enhance the coating rate and release performance. The adhesive and tensile characteristics of the modified polyurea binder, as well as the granule properties of modified polyurea binder potassium chloride, were studied to determine the ideal lignin-grafted ratio. The effect of the modified polyurea binder with potassium chloride on the properties of coated fertilizer was investigated. The findings, shown by radar maps of the binder's properties, demonstrated that the ideal mass ratio of the modified lignin polyurea binder to urea is 1:2. The Fourier-transform infrared spectroscopy results demonstrated that the amino functional groups of lignin were enhanced, improving the product's interfacial compatibility with the polyurea matrix. Compared to humic acid (HA; 12%) and bentonite (Ben; 30%) treatments, the granule intensity of the 9.9%—1:2 treatment considerably increased by 139.10% and 38.86%, respectively, while the static angle of the granules reduced by 16.67% and 3.81%. The 28-day cumulative release rate of the modified polyurea (9.9%—2:1) with a 5% coating thickness was the lowest (28%), 42% lower than that of the lowest conventional treatment. In summary, the creation of a bio-lignin polyurea binder under the optimum conditions reduced the need for petrochemical-based materials, allowed the preparation of fertilizer with granules of increased fluidity, and enabled the successful coating of a high-salt potassium fertilizer, offering a novel technique for the high-value application of potash fertilizer coating.

**Keywords:** lignin; modified polyurea; binder; potassium chloride; controlled-release fertilizer



**Citation:** Li, M.; E, G.; Wang, C.; Shi, R.; Wang, J.; Wang, S.; Wang, Y.; Chen, Q.; Li, Z.; Liu, Z. Synthesis and Application of Modified Lignin Polyurea Binder for Manufacturing a Controlled-Release Potassium Fertilizer. *Agronomy* **2023**, *13*, 2641. <https://doi.org/10.3390/agronomy13102641>

Academic Editor: David Fangueiro

Received: 26 September 2023

Revised: 11 October 2023

Accepted: 16 October 2023

Published: 19 October 2023



**Copyright:** © 2023 by the authors. Licensee MDPI, Basel, Switzerland. This article is an open access article distributed under the terms and conditions of the Creative Commons Attribution (CC BY) license (<https://creativecommons.org/licenses/by/4.0/>).

## 1. Introduction

Potassium is one of the three main nutrients for crop growth [1,2] and is primarily derived from potash fertilizers. About 90% of the potassium produced by human societies is used in the production of chemical fertilizers. The world is extremely rich in potassium resources, but their distribution is uneven. Potassium resources are controlled by several major producer countries, including Canada, Russia, Belarus, and Germany, which together hold 92% of the world reserves [3]. However, some countries, unable to produce sufficient quantities of potash fertilizer to meet their demands for agricultural development, are largely dependent on imports. As such, potash prices are highly vulnerable to fluctuations in international market prices [4]. Affected by the supply of bulk materials, the cost of fertilizer raw materials has sharply risen and remains high, putting economic pressure on actors ranging from farmers to grow crops [5]. Therefore, the tasks of developing and

popularizing potash fertilizer alternatives, improving the utilization rate of potash fertilizer, and optimizing fertilization technologies and management are crucial for the sustainable development of agriculture [6].

The use of controlled-release fertilizers (CRF) can improve fertilizer utilization, reduce environmental pollution [7,8], save labor, and improve crop yield and quality [9]. There have been several studies on controlled-release potash fertilizers to date, and the extant research on traditional potash fertilizer is more extensive [10,11]. With 85–90% of the market share for potash fertilizer products, potassium chloride (KCl) is the most popular potash fertilizer product globally [12]. Additionally, the amount of membrane material used and released is significantly influenced by a coated fertilizer core [13]. The creation of a fertilizer core with exceptional properties is, thus, a pressing current priority.

Powdered granular crystal potassium chloride lacks viscosity and plasticity. Compared with conventional controlled-release urea, the difficulty in core preparation is the key challenge in the development and use of coated potassium chloride fertilizer [14]. Extrusion granulation and agglomeration granulation are the two primary granulation techniques for potash fertilizer [15]. The extrusion granulation method has the disadvantage of poor roundness [16]. The agglomeration granulation method, also known as the turntable granulation method, has the advantages of straightforward production conditions, uniform granulation, a low amount of return material, and a high output capacity [17,18]. The method of agglomeration granulation generally involves mixing, diffusion of the binder, aggregation, combination, friction, crushing, and drying—a total of seven steps [19]. Viscous material plays a leading role in this granulation process as the determinant of fertilizer granule strength [20,21]. Fertilizer granules with a low mechanical strength are fragile during transportation, storage, and fertilization. Therefore, the strength of the fertilizer granules is also an important indicator for evaluating the suitability for mechanical fertilization [14,22,23].

Inorganic binders, including lime, sodium silicate, and other materials, are broadly used in multitudinous products owing to their outstanding physicochemical performance [24,25]. In fertilizer granulation, inorganic binders can solve puzzles that involve a low hardness, a low balling rate, a high moisture content, and a large budget of products [26]. While extensive applications of mineral binders result in the nutrient content of the finished granular products being relatively low, this is worsened by the fact that relatively large additions cause serious pollution during the process [27].

Pectin, rubber, starch, and other natural substances make up the primary organic binder. With the development of industry, natural organic binders cannot satisfy the demands of industrial operations [28]. Chemical synthetic alternatives proliferated after the development of natural organic adhesives. Urea–formaldehyde binder compound fertilizers have the advantages of a long fertilizer effect, good storability, and environmentally friendly behavior [29]. However, the cost of urea–formaldehyde binder compound fertilizers is too high, the research and development of the production process lacks innovation, and the preparation process of formaldehyde (FA) can cause safety issues [30]. Historically, starch was generally used in the binder due to its extensive material sources, low cost, and environmental friendliness [31]. In contrast with most conventional synthetic polymers, starch-based materials possess weak mechanical characteristics and low water sensitivity [32,33]. In the 1980s, the Texaco Company produced polyurea via the combination of the epoxy curing agent terminal amino polyether and isocyanate resin [34]. Polyurea was employed as the strong bonding material because of its strong polar functional group, fast curing speed, and exceptional moisture resistance and the absence of requirements for its catalyst and solvent [35–39]. Polyurea was derived from non-renewable petrochemical resources and, as such, became more expensive than other traditional binders [40]. Taking into account the growing shortage of petrochemical resources, it became imperative to develop technology capable of relieving the stress of raw materials in polyurea production. Lignin is the largest natural aromatic biopolymer with rich hydroxyl groups, a low production cost, and eco-friendly behavior [41]. The global production of industrial lignin,

a by-product of the paper and hydrolysis industries, is 15 billion tons per year, yet the majority is burned or leached into the environment as wastewater, posing a serious threat to the environment in the course of processing [42]. Hence, this study uses lignin to create a kind of eco-friendly lignin-based polyurea binder to reduce the use of petrochemical resources for polyurea and consume surplus lignin.

In this study, a novel type of controlled-release potassium chloride fertilizer core is designed and prepared based on the above considerations. (1) Differential scanning calorimetry (DSC), thermal gravimetric analysis (TGA), and Fourier-transform infrared spectra (FTIR) are used to investigate the functional properties of the lignin-based polyurea binder. (2) The fertilizer granule strength, the fluidity, and hygroscopicity trials are obtained to analyze the optimal urea and lignin ratio for the lignin–polyurea binder. (3) The interaction among the material, the coating, and the fertilizer nutrient release characteristic is assessed via measuring the fertilizer release rate, scanning electron microscopy (SEM), and high-precision laser scanning.

## 2. Materials and Methods

### 2.1. Materials and Reagents

Potassium chloride (in the form of white powder) was purchased from Beijing Zhong hua Fertilizer Co., Ltd. (Beijing, China). Dealkalized lignin was provided by Shanghai Source Leaf Biotechnology Co., Ltd. (Shanghai, China). Polyetheramine D2000 (D2000), formaldehyde, and N, N-dimethylacetamide (DMAC) were obtained from Aladdin Industrial Co., Ltd. (Shanghai, China). Isophorone diisocyanate (IPDI) and diethyl toluene diamine were supplied by Shanghai Macklin Biochemical Co., Ltd. (Shanghai, China). Urea, sodium hydroxide, bentonite, and calcium superphosphate were purchased from Tianjin Kaitong Chemical Reagent Co., Ltd. (Tianjin, China).

### 2.2. Preparation of Urea-Grafted Lignin and the Determination of Lignin-Grafted Ratio

Urea-grafted lignin was prepared using the Mannich reaction, as shown in Table S1. First, 10 g of lignin was dissolved in 500 mL 2% NaOH solution; the mixture was added to 500 mL three-necked flask under mechanical agitation, heated to 50 °C, and then stirred for 1 h in order to ensure the lignin was fully dissolved. Next, 10 g of urea was added, and the mixture was stirred for 1 h to completely mix with the lignin. A 37% formaldehyde solution was dropwise added to the flask while stirring when the temperature was raised to 80 °C. After 2.5 h, the solution was acidified using 20% H<sub>2</sub>SO<sub>4</sub>. The precipitated product was washed with pure water, filtered, and vacuum-dried at 75 °C for 24 h. Ultraviolet (UV) spectrophotometry was applied to detect the lignin concentration of the sample solution (100 mg L<sup>-1</sup>) at the wavelength of 280 nm (the distinctive absorption band of the benzene ring). Absorption intensities at 280 nm of lignin solutions with concentrations of 0, 20, 40, 60, 80, and 100 mg L<sup>-1</sup> were fitted to acquire the standard absorption curve of a lignin solution. As shown in Table S2, the lignin-grafted rates in the samples of urea-grafted lignin were calculated according to the standard absorption curve.

### 2.3. Preparation and Characterization of Lignin Modified Polyurea Binder

Prepolymerization and chain extension were the two main steps in creating the lignin-containing polyurea binder. The flask containing D2000 was first filled with IPDI in order to form the prepolymer under constant stirring for 1 h at room temperature. In the subsequent phase, the urea-grafted lignin (or the chain extender bis (4-aminophenyl) and disulfide) and the solvent DMAC were mixed and poured into the prepolymer, undergoing agitation at room temperature for 0.5 h. After the homogeneous solution was obtained, it was put into a glass for subsequent usage, as shown in Table S3.

The grafted lignin and the modified binder were identified using a Fourier-transform infrared spectrometer (Tango-R FTIR, Tai'an Kaijie Instrument and Equipment Co., Ltd., Tai'an, China). FTIR examination was conducted with a resolution of 4 cm<sup>-1</sup> and 32 scans over a wave-number range of 400–4000 cm<sup>-1</sup> using Cu K $\alpha$  radiation. The adhesive values

of binders were measured using a digital rotating viscometer (LVDV-II + Pro, Middleboro, MA, USA) at 120 rpm at 120 °C and 25 °C. A microcomputer-controlled electronic universal testing machine (UTM6202X, Shenzhen Sansi Crossbar Technology Co., Ltd., Shenzhen, China) was utilized to determine the tensile strength and elastic modulus of the binder. The universal material testing apparatus (Y (G) B028E-1000, Wenzhou Darong Textile Instrument Co., Ltd., Wenzhou, China) was introduced to assess the dry bonding strength of the binder. The thermogravimetric analysis of the binder was carried out using a thermogravimetric analyzer (Netzsch Sta 449F3, Netzsch, Selb, Germany). Differential scanning calorimetry (DSC, SERIES2000, Mettler Toledo, Columbus, OH, USA) was used in the thermal evaluation of the modified binders.

#### 2.4. Preparation of Fertilizer Cores

Humic acid, bentonite, superphosphate, and potassium chloride were weighed, crushed, and sieved through a mesh size of 100. The materials were thoroughly mixed and poured into a homemade disc granulator [43]. At that point, the binder accounted for 3.3–9.9% of the fertilizer by weight. The binder solution was gently sprayed onto the pelletizer disc material using a mini-type atomizer. Table S4 shows the different binders and the proportions in which they were added. Subsequently, quantitative water was added to the atomizer and slowly sprayed onto the material at a steady pace. When the powder was fully formed into particles, the granules continued to roll in the disc for 5 min, making it more uniform, rounded, and compact. The granules were screened to produce 2–5 mm fertilizer, and the <2 mm material continued to be granulated in the granulator. The >5 mm granules were crushed and then granulated again, undergoing 4 cycles of the process. Then, the suitable fertilizer granules were heated in the oven at 105 °C to 110 °C until reaching a constant weight.

#### 2.5. Evaluation of Fertilizer Coating Effect

Three different types of fertilizer cores involving lignin-based polyurea potassium chloride (PGL1:1, PGL1:2, and PGL2:1), bentonite potassium chloride (Ben), and conventional potassium chloride (HN; irregular solid shape) were analyzed in this work. Soybean oil-based polyurethane (OBPU) was chosen as the coating, and its thickness reached 4% and 5% of the mass of the fertilizer. After 2–5 mm potassium fertilizer granules (1 kg) were added into a rotating drum and preheated at 80 °C for 20 min, 5 g of polyolefin wax was uniformly spread onto the surface of potassium fertilizer granules, and the reactants were mixed for approximately 5–10 min. OBPU was evenly sprayed onto the waxy potassium fertilizer and heated at 80 °C for 5–30 min. The mixture accounted for about 1% of the fertilizer mass each time [44]. The release rate of coated fertilizer was determined via the addition of coated fertilizer (10 g) in a test bottle containing 200 mL of deionized water. The conductivity of the solution samples was determined using a conductivity meter (PC 700, Thermo Fisher, Singapore) at regular intervals until the cumulative K release exceeded 80% [13]. The cumulative K release rates were determined with Equation (1):

$$v_t = w_t / w \times 100 \quad (1)$$

where  $v_t$  is the cumulative K release rate during a specific period (days),  $w_t$  (S/m) is the mass of K released during the period, and  $w$  (S/m) is the initial mass of total K.

Scanning electron microscopy (SEM, Zeiss Gemini 300, Oberkochen, Germany) was used to examine the surface and cross-sectional morphology of the treated fertilizers. We compared the three-dimensional profile and specific surface area of HN potassium chloride and lignin-based polyurea potassium chloride using high-precision laser scanning equipment (CMM Zeiss Spectrum II, Oberkochen, Germany).

#### 2.6. Characterization of Fertilizer Core Granules

The roundness and granule diameter distribution of fertilizers were measured using a 3D granule size analyzer (AP0078, Heze Jinzhengda Ecological Engineering Co., Ltd., Heze,

China). A granule strength tester (YHKC-2 a, Yinhe Instrument Factory, Taizhou, China) was adopted to gauge the hardness of fertilizer. The angle of repose, an indicator of granule fluidity and roundness, was the slope measured at the bottom of a pile of uncompressed particulate solids at the time of runoff occurrence [45,46]. The larger the angle of repose was, the lower the granule fluidity was; whereas the smaller the angle of repose was, the higher the granule fluidity became [44]. A fertilizer sample of 100 mL was placed into the funnel of a repose angle tester (FBS104, FURBS Instrument Co., Ltd., Shenzhen, China), and the fertilizer accumulation height (mL) ( $h$ ) was measured. The angle of repose ( $\Phi$ ) was calculated by Equation (2):

$$\Phi = \frac{\left( \arctan \left( \frac{h}{5} \right) \right) 180}{\pi} \quad (2)$$

In this procedure, 10 g of fertilizer was precisely weighed and cultivated in an incubator at a constant temperature (the temperature was set at 25 °C, and the relative humidity was set at 60%). Then, it was weighed every 0.5 h to calculate the fertilizer hygroscopicity.

$$W = \frac{B - G}{G} * 100\% \quad (3)$$

where  $W$  (%) is the hygroscopicity,  $B$  (g) is the fertilizer weight after hygroscopicity, and  $G$  (g) is the fertilizer weight before hygroscopicity.

### 2.7. Flowchart of the Modified Polyurea Binder Controlled-Release Potassium Chloride Process

Figure S1 displays the flowchart of the modified polyurea binder controlled-release potassium chloride process. This process included lignin grafting, polyurea modification, disc granulation, and coating—a total of 4 steps.

### 2.8. Statistical Analysis

All data were subjected to analysis of variance (ANOVA) using SPSS Statistics Version 20 for Windows (IBM Corporation, Armonk, NY, USA). Graphs were plotted using SigmaPlot 12.5. Differences were considered significant at  $p < 0.05$ .

## 3. Results and Discussion

### 3.1. Synthesis of Modified Lignin-Based Polyurea Binder

The lignin polyurea binder was synthesized by modifying lignin (L) with urea through the Mannich reaction, which introduced highly active amino groups into the lignin [47]. Figures 1a and 2a demonstrate the formation of lignin-containing polyurea binders. In this process, the amino groups increased the reactivity of lignin with the isocyanate group and improved interfacial compatibility between lignin and the polyurea matrix.

The compositional structure of urea-grafted lignin (GL) was determined via FTIR, as shown in Figure 1b. In contrast to the original lignin, the spectra of GL had one absorption peak around 1080  $\text{cm}^{-1}$ . This was ascribed to the C–H bond, and the absorption peak of the C–O–C bond appeared at 1025  $\text{cm}^{-1}$  in urea. The strength of the characteristic peaks at 2930  $\text{cm}^{-1}$  and 2840  $\text{cm}^{-1}$ , attributed to the dissymmetric and symmetric stretching of  $-\text{CH}_3$  and  $-\text{CH}_2-$ , respectively, significantly increased in urea-grafted lignin. The FTIR patterns of samples verified that the urea was successfully grafted onto the lignin molecules. In addition, the C=O vibration in the amino acyl group in GL occurred at 1670  $\text{cm}^{-1}$ , indicating that the  $-\text{NCO}$  group was successfully transformed into  $-\text{NH-CO-NH}-$ . Peaks occurred at 2252  $\text{cm}^{-1}$  due to the vibration in the  $-\text{NCO}$  group in IPDI and disappeared in GL. Figure 2b shows the FTIR patterns of polyurea binders with different lignin ratios, and the spectra were similar. The peaks at 3444  $\text{cm}^{-1}$  and 3336  $\text{cm}^{-1}$  represented the stretching vibration of  $-\text{OH}$  in lignin and  $-\text{N-H}-$  in urea bonds, respectively [48]. The absorption peaks at 3120  $\text{cm}^{-1}$  and 3000  $\text{cm}^{-1}$  belonged to the aromatic C–H bond vibration. Due to the bending vibration of  $-\text{N-H}-$  and the aromatic skeleton vibration of lignin, the C=O bond could be observed at 1670  $\text{cm}^{-1}$  and 1604  $\text{cm}^{-1}$ . The absorption peaks at

1448  $\text{cm}^{-1}$  and 1380  $\text{cm}^{-1}$  were caused by the vibration of the C–N bond in the urea group. The absorption peaks appeared around 1165  $\text{cm}^{-1}$  and 1270  $\text{cm}^{-1}$ , corresponding to the asymmetric bending of C–O. These observations demonstrated that the lignin-containing polyurea binder was successfully synthesized.

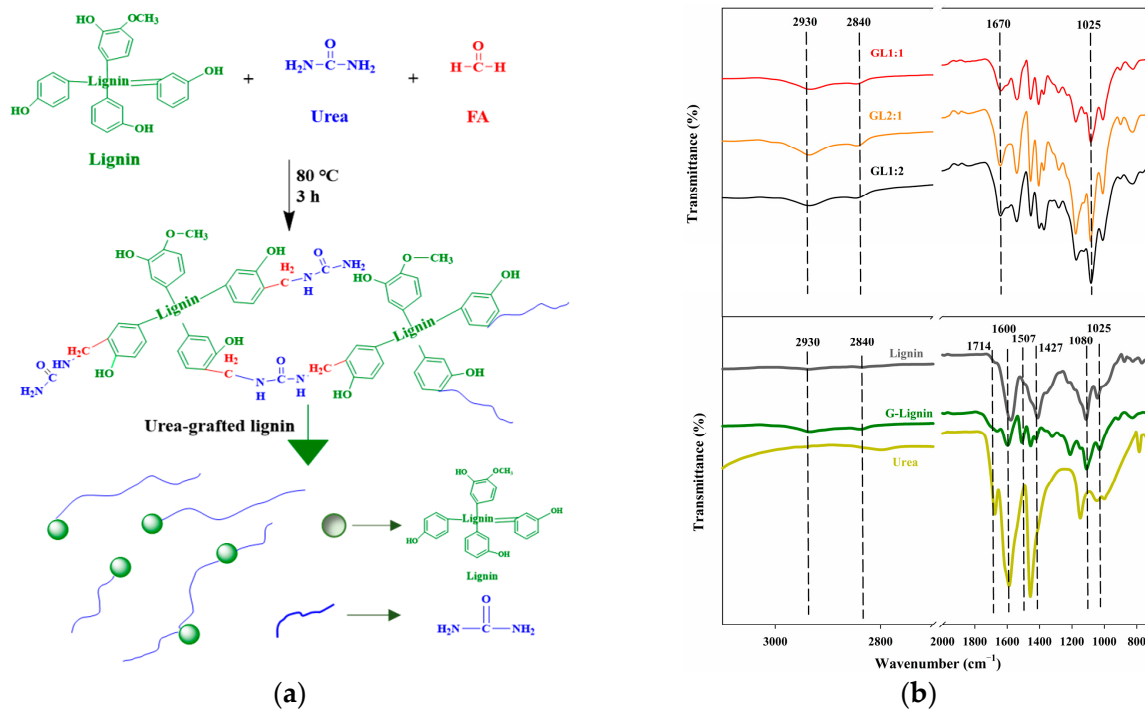


Figure 1. Synthesis process of urea grafted lignin (a) and the FTIR spectra of lignin, urea, and urea-grafted lignin (GL1:1, 1:2, and 2:1) (b).

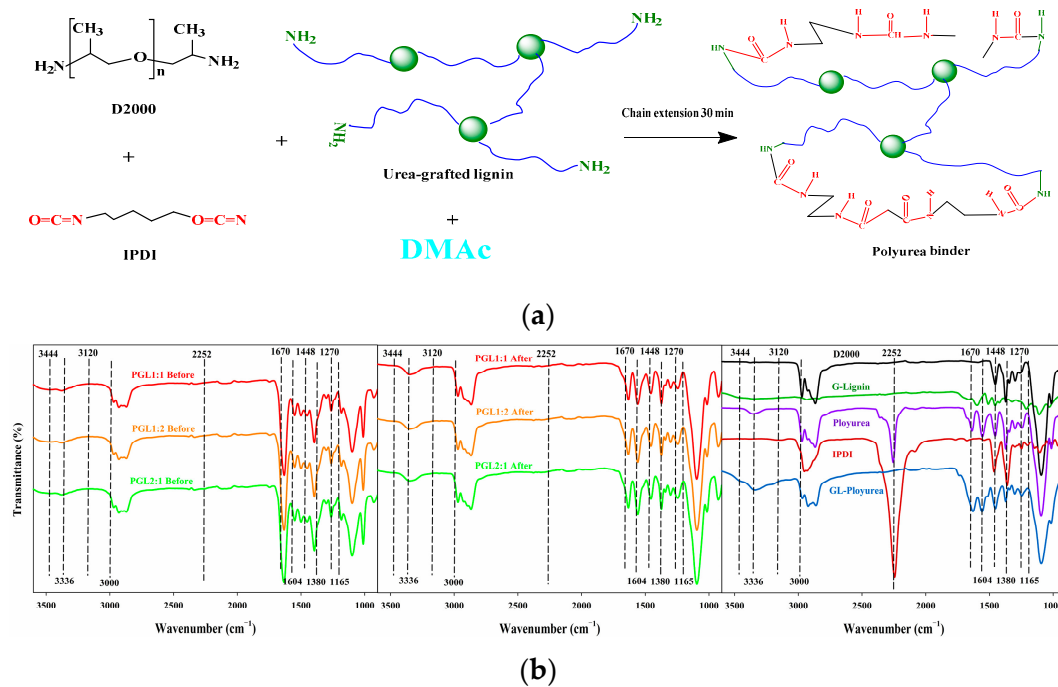
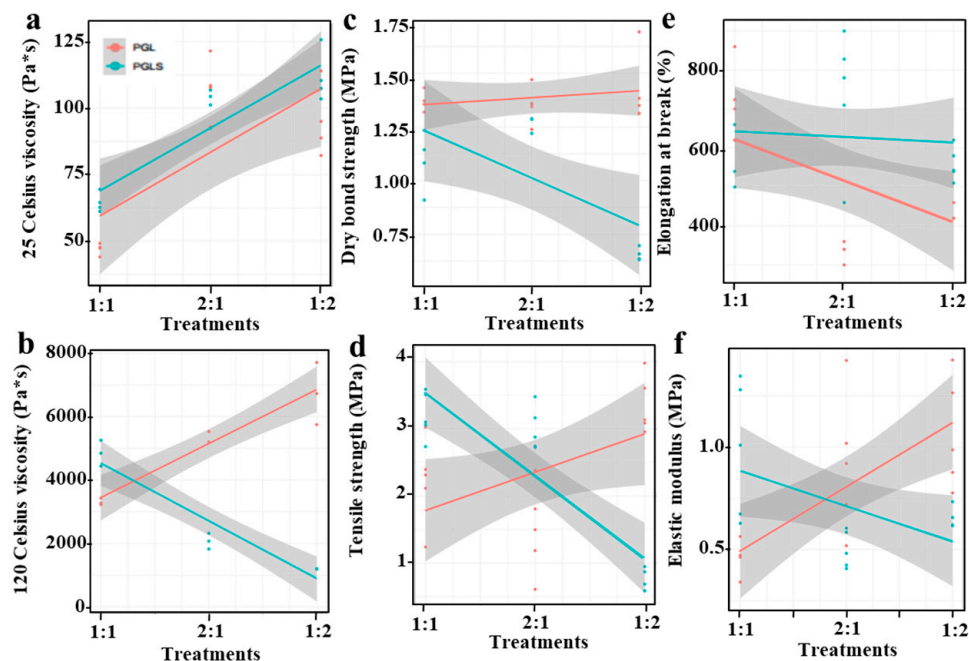


Figure 2. Synthesis process of lignin-based polyurea binder (a) and the FTIR spectra of D2000, IPDI, polyurea, urea-grafted lignin, and urea-grafted lignin polyurea (PGL1:1, 1:2, and 2:1) (b).

### 3.2. Performance Characterization of Modified Lignin-Based Polyurea Binder

Property analysis for modified lignin-based polyurea binders is presented in Figure 3. The viscosity of lignin-based polyurea improved with the increase in temperature from 25 °C (Figure 3a) to 120 °C (Figure 3b). The 120 °C viscosity (Figure 3b), dry bonding strength (Figure 3c), tensile strength (Figure 3d), and elastic modulus (Figure 3f) of PGL (1:2) treatment were higher than those of PGLS (1:2) treatment by 458.3%, 100%, 113.6%, and 110.9%, respectively. This was likely because disulfide bonds increased the spatial mobility of the modified polyurea molecules, which reduced the viscosity, dry bonding strength, tensile strength, and elastic modulus at 120 °C. Further PGLS treatments outperformed PGL treatments in terms of elongation at break (Figure 3e), which might be due to the high-stability di-sulfide bonds owning a solidly covalent bond nature.



**Figure 3.** Characterization diagram of lignin-based polyurea binder: 25 Celsius viscosity (a), 120 Celsius viscosity (b), dry bond strength (c), tensile strength (d), elongation at break (e), and elastic modulus (f). PGL polyurea binder containing grafted lignin; PGLS represents polyurea binder containing grafted lignin and disulfide; \* represents for multiplication sign.

### 3.3. TGA and DSC Analysis of Lignin-Based Polyurea Binder

The thermal stability of the modified lignin polyurea binder was studied via thermogravimetric analysis. Figure S2 displays the TGA curves. The typical temperatures of  $T_{5\%}$ ,  $T_{50\%}$ , and  $T_{max}$  are shown in Table S5. The  $T_{5\%}$  in the modified lignin with a disulfide bond (PGLS1:1, PGLS1:2, and PGLS2:1) was comparable to that in PL, suggesting that the introduction of disulfide bond made no difference to the initial thermal degradation temperature of the polyurea binder. In the PGL treatment,  $T_{5\%}$  gradually increased with the increase in lignin content, and the  $T_{50\%}$  and  $T_{max}$  of polyurea binders containing lignin were higher than those of PGLS, showing that the disulfide bond could weaken stability while aromatic lignin could increase it. The research of Fang et al. also showed the same results [47].

The DSC reheating curve of the polyurea coating is shown in Figure S3. The glass transition temperature of the polyurea coating with the increase in lignin content indicates that the fluidity of the polyurea chain decreased due to the hydrogen bond interaction between lignin and the polyurea matrix.

### 3.4. Granule Strength and Fluidity of Modified Polyurea Potassium Chloride Fertilizer Cores

The granule strength of fertilizer cores was a vital parameter in assessing their practical application. Therefore, the granule strength of different binder fertilizers was detected, as shown in Figure 4a. The fertilizer granule strength of modified polyurea binders with an average strength of 35.8 N was the highest under the conditions of adding different fertilizer binders. The granule strength of fertilizer post-treatment with pure water was only 10.7 N, and the hardness of the modified treatment was 3.3 times that produced via the water treatment. Compared with 12%—HA and 30%—Ben treatments, the intensity of the 9.9%—1:2 treatment increased considerably by 139.10% and 38.86%, respectively, because of the network structure formation of cross-linked polyurea binder within the fertilizer granules during the granulation process. The results of Yang et al. showed that the formation of polyphosphate and its cross-linking with montmorillonite significantly enhanced the particle strength of the fertilizers [43]. As the fertilizers were heated and dried, the viscosity increased, and the granules became more compact. Figure 4b showed the effect of different modified polyurea binder proportions on the fertilizer granule strength. After adding the modified polyurea binder, the highest granule strength of PGL treatments belonged to PGL 9.9%—1:2, of which the average strength reached 35.8 N. This was higher than that achieved with other treatments by a significant degree. Conversely, in PGLS treatments, PGLS 9.9%—2:1 had the highest granule strength, and the average strength reached 23.8 N. The reason for this was that the addition of disulfide bonds not only increased fluidity but also reduced viscosity, resulting in a lower granule strength of the fertilizer.

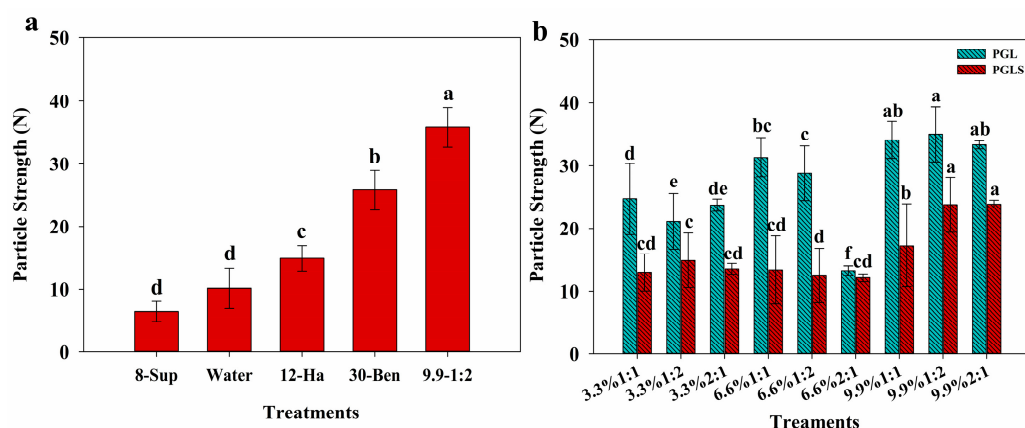


**Figure 4.** Comparison of granule strength of different binder fertilizers (a), comparison of fertilizer granule strength with different proportions of modified polyurea binder (b). Note: same letters for the bars indicate that means of fertilizer granule strength were not significantly different among treatments at 5% level.

The slip angle and rest angle, as the two important indicators used to evaluate the flowability of fertilizers, are revealed in Figure 5a,b. To eliminate the error caused by moisture, the fertilizer was baked in an oven at 105 °C for 24 h before the test. It was then placed into a drier for the determination to be carried out. The fluidity was inversely correlated with the slip angle and rest angle of the materials. When the angle was smaller, the friction of materials was smaller, and the fluidity increased. The PGL1:2—9.9% treatment showed minimum angles of 15.3° and 15.5°, which were 44% and 38% lower than those of conventional HN potassium chloride, respectively. The PGL1:2—9.9% treatment possessed excellent fluidization performance, improving the transportation efficiency and prolonging the preservation time of fertilizers.

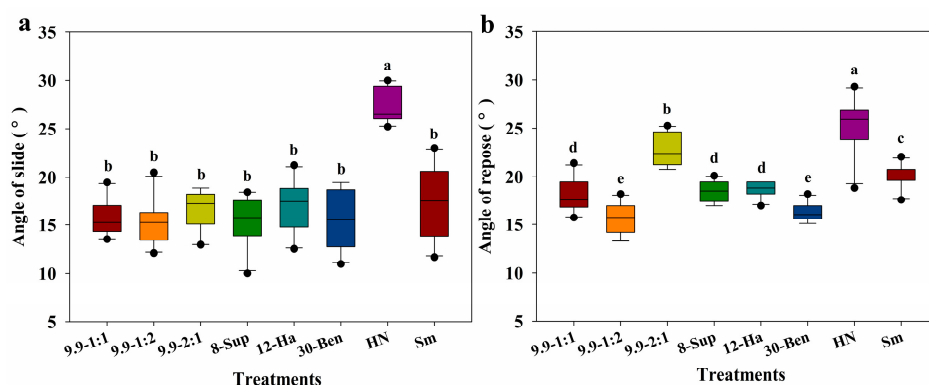


**Figure 5.** Sliding angle of granules of potassium chloride fertilizer (a), granule resting angle of potassium chloride fertilizer (b) (Sm stands for commercially available potash). Note: same letters for the boxes indicate that means of sliding angle and resting angle of granules were not significantly different among treatments at 5% level.

### 3.5. Radar Image of Lignin-Based Polyurea Binder

According to the radar diagram shown in Figure 6, it can be seen that the PGL1:2 treatment was superior to other treatments in terms of viscosity and tensile strength. The quantitative classification of radar images is provided in Table S6. In particular, the strength of fertilizer granules was directly assessed by determining the degree of cross-linking between the binder and fertilizer. This was consistent with the findings of Dhenge et al. [49]. The viscosity was the essential parameter influencing fertilizer granule strength, controlling the degree of cross-linking between the binder and fertilizer. The PGL1:2 had the most remarkable and comprehensive performance, despite its index of elongation at break being at a moderate level. The PGL1:2 treatment was more circular than the others, which indicated that the PGL1:2 treatment had better coordination of the evaluation indexes.

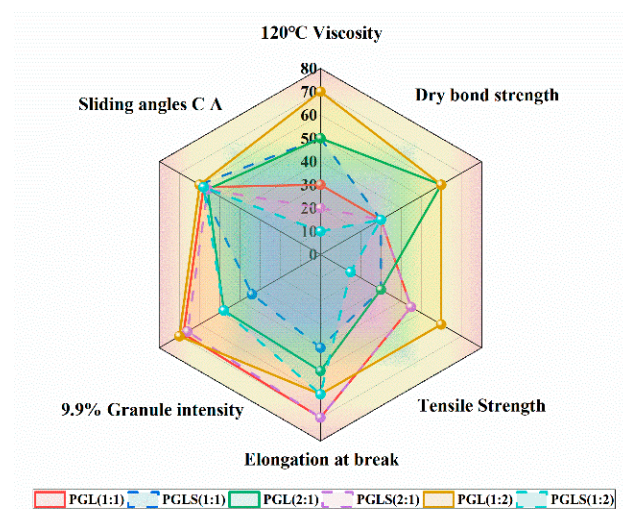


**Figure 6.** Radar diagram of synthetic properties of lignin-based polyurea binders. Sliding angles C A represent the supplementary angle of the sliding angle.

### 3.6. Analysis of Granule Size and Roundness of Coated Potassium Chloride Fertilizers and Fertilizer Cores

Figure 7 displays the granule size distribution of uncoated and 4% OBPU-coated potassium chloride. PGL2:1 treatment of uncoated granules, with the diameter ranging from 3.0 to 5.0 mm, accounted for 96.89% of the total. This was the highest proportion among all the experimental treatments. The granule diameters of the PGL1:1, PGL1:2, Ben, and HN treatments were 93.57%, 95.80%, 87.69%, and 76.91%, respectively. More than 90.0% of the fertilizer with lignin-binder produced granules 3.0–5.0 mm in diameter. The

diameter of granules with the highest proportion of PGL2:1 treatment ranged from 3.4 to 4.2 mm, accounting for 28.25%. The granules (diameter of 3.0–5.0 mm) in the PGL2:1 treatment after the coating test accounted for 96.79% of the total, which was also the highest among all treatments. It was demonstrated that the addition of a certain degree (equivalent to 9.9% of the fertilizer mass) of the lignin-based polyurea binder could make the granule diameter more uniform and more conducive to uniform coating with the liquid.

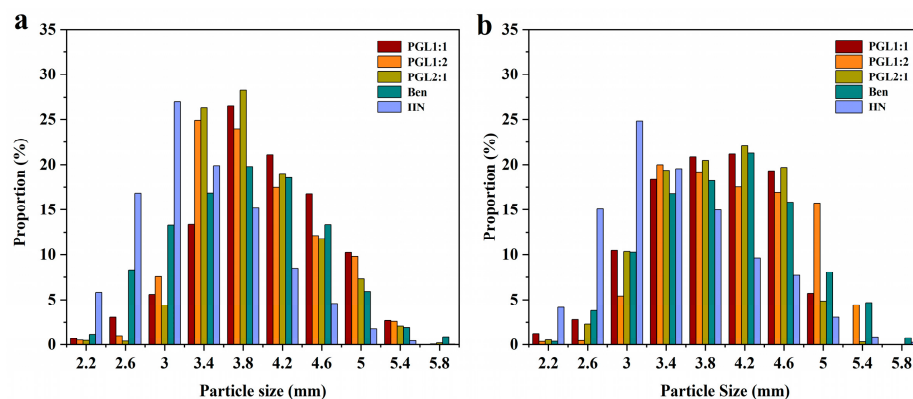


**Figure 7.** Granule size distribution of uncoated potassium chloride fertilizer (a) and 4% OBPU-coated potassium chloride fertilizer (b).

HN potassium chloride had the worst roundness of all the treatments, showing irregular polyhedral shapes, and the results are shown in Figure S4. The granules were not suitable for the fertilizer core granules used in the coating treatment because the uneven coating membrane on the surface of fertilizer granules represented a poor release capacity. PGL 2:1—9.9% processing possessed the best roundness and was beneficial for the coating processing.

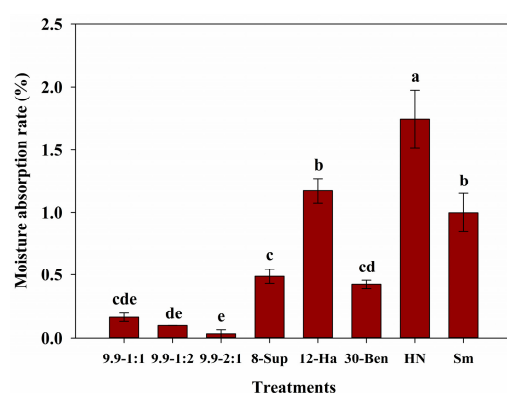
### 3.7. Hygroscopicity of Potassium Chloride Fertilizer Cores

Figure 8 reports the moisture absorption rates of potassium chloride fertilizers with the different binders used in this study. Generally, the standard moisture absorption rate of potassium chloride should be below 0.3%. The moisture absorption rates of PGL2:1, PGL1:1, and PGL1:2 were 0.03%, 0.16%, and 0.10%, respectively, which were all up to standard. This occurred because the partially modified polyurea binder was coated onto the fertilizer granules surface, forming a hydrophobic membrane with moisture resistance, whereas the moisture absorption rates of the remaining treatments were all above 0.3%. HN treatment had the highest moisture absorption rate of 1.7%, a level far above the standard moisture absorption rate. The reason for this was that there was no hydrophobic substance on the surface after HN treatment, as some granules would desquamate, exposing the internal structure. The desquamate section became irregular, increasing the water absorption capacity and the moisture absorption rate of the fertilizers.

### 3.8. Nutrient Release Rate of Potassium Chloride Granules with Different Membrane Thickness

According to the international standard for controlled-release fertilizers (Release of the first slow and controlled release fertilizer industry white paper, 2016; ISO 18644:2016), the initial release rate of CRF should be under 15%, and the cumulative nutrient release within 28 days should not surpass 75%. For the 4% and 5% coating thickness treatments, the initial release rates of PGL1:1, Ben, and HN were 25.75%, 50.98%, and 46.79% and 25.32%, 28.26%, and 42.18%, respectively. These rates did not conform to the aforementioned international standards, as illustrated in Figure 9. A plausible reason for this anomaly is the reaction of potassium ions with isocyanate, leading to the formation of urea formate. This compound subsequently establishes a three-dimensional network structure among the polyurethane molecules, restricting the fluidity and elasticity of the polyurethane

chains [50]. Moreover, in the presence of potassium ions, several isocyanate molecules might undergo condensation reactions, leading to the creation of a biuret group. This process potentially culminates in gel formation. An excess of potassium ions, however, can expedite the polyurethane gelation process, causing uncontrolled reactions that jeopardize the product's performance and quality [51]. The interaction between potassium ions and functional groups in the coating, such as hydroxyl and amine groups, can result in the formation of complexes or induce ion exchange due to intense charge attraction. Such interactions might compromise the bond between coating molecules, thereby diminishing the adhesion between the coating and its substrate [52]. In environments characterized by high salinity, chloride ions might react with isocyanates or polyols in the coating, yielding novel compounds. Such reactions can consume the polymer constituents of the coating, disrupting the curing process and diminishing the coating's hardness [53]. Collectively, these factors could detrimentally affect the formation of the polyurethane membrane and may even result in fertilizers failing to comply with standard usage requirements.



**Figure 8.** Moisture absorption rate of potassium chloride fertilizer with different binders. Note: same letters for the bars indicate that means of moisture absorption rate were not significantly different among treatments at 5% level.

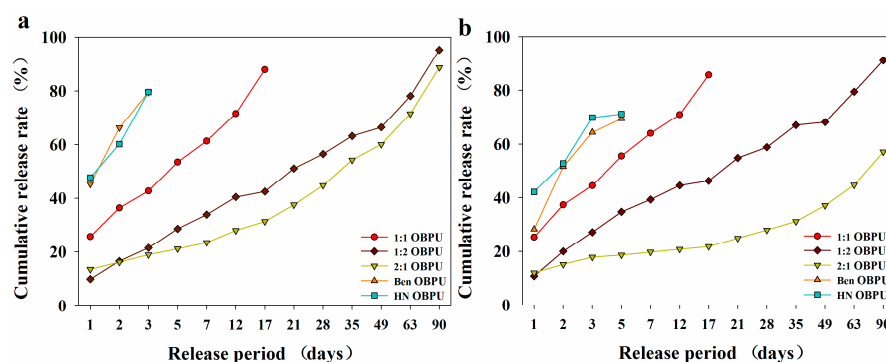


**Figure 9.** Cumulative release rate of coated potassium chloride fertilizer with different thickness: 4% coating fluid (a) and 5% coating fluid (b).

Experimental outcomes revealed that the most effective treatment, Ben-5%-OBPU, exhibited an 80% release rate over just 5 days of spherical bentonite exposure. This behavior might be attributable to the inherent composition of bentonite, a water-bearing clay ore primarily composed of montmorillonite. Within this structure, high-valence silicon and aluminum ions are amenable to replacement using other lower-valence cations [54]. Such substitutions provide a negative charge to montmorillonite, empowering it with the propensity to adsorb certain cations. Intriguingly, these interlayer cations also exhibit pronounced hydration characteristics, allowing montmorillonite to adsorb a water volume ranging from 8 to 20 times its original volume into its interlayers and even expand up to 30-fold. As a consequence, the encapsulated fertilizer core undergoes an expansion in volume

and a reduction in thickness and, in some instances, can even rupture the encapsulating membrane. The post-coating release efficiency, therefore, is less than optimal.

The performance of various lignin-based binders exhibited a noticeable difference when subjected to PGL2:1, PGL1:2, and PGL1:1 treatments. Notably, the PGL2:1 treatment, which employed different proportions of binders, demonstrated the most favorable results, with a coating thickness of 5%. Its initial release rate stood at 12%, while the cumulative release rate over 28 days reached 28%, seamlessly aligning with international standards. Conversely, the PGL1:2 treatment recorded an initial release rate of 10.82% and a 28-day cumulative release rate of 58.80%. The PGL1:1 treatment yielded an initial release rate of 25.31%, which unfortunately did not conform to international guidelines. This variance in results might be attributed to the interaction of lignin's structure with polyurethane. Lignin comprises benzene and toluene rings, alongside an assortment of functional groups [55]. The benzene ring, possessing numerous hydroxyl groups, can cross-link with other lignin molecules and proteins. Significantly, isocyanates have the potential to react with hydroxyl groups, not only culminating in a polyurethane coating on the fertilizer core [56] but also enabling binder cross-linking. This results in a denser internal matrix, which further impedes the fertilizer's release rate. Furthermore, the inclusion of urea as a chain extender can enhance the mechanical and thermal properties of polyurethane, augmenting its resistance to abrasion, weathering, and chemical corrosion. In the context of the lignin-based polyurea binder, it is modified by urea. The PGL1:2 treatment had the highest urea content due to the maximal lignin content in the PGL2:1 treatment, where lignin predominantly constituted the binder. Consequently, among the experimental treatments, PGL2:1 emerged as the most effective, sequentially followed by PGL1:2 and PGL1:1.

### 3.9. Fourier-Transform Infrared Spectrum of Membrane Shell of Controlled-Release Potassium Chloride Fertilizers

As shown in Figure 10, the structure and composition changes in the coatings were confirmed via FTIR. Within  $3200\text{--}3500\text{ cm}^{-1}$ , there was a strong and wide absorption peak representing the O–H stretching vibration band. In contrast, the O–H peak intensity of the bentonite binder was lower than that of polyurea binder treatments, indicating that the bentonite binder made the hard microstructure of the coating begin to loosen. The bands in the range of  $2800\text{--}2932\text{ cm}^{-1}$  appeared because the stretching vibration of C–H and the peak intensity of polyurea binder treatments decreased compared with those of the bentonite binder treatment due to the weakness of the C–H stretching vibration. The sharp absorption peak at  $1590\text{ cm}^{-1}$  was formed via the C–C stretching vibration in terms of aromaticity. It was much more intense in the membrane shell of modified polyurea binder fertilizers than that of bentonite binder fertilizers as the benzene ring was more stable with polyurea binders. The strong absorption peak of polyurethane near  $1720\text{ cm}^{-1}$  was attributed to the tensile vibration of C–O, and its attenuation manifested the oxidative degradation of membrane material. One peak shift near  $1057\text{ cm}^{-1}$  (the C–O tensile vibration induced by N–CO–O) also showed a change in the polyurethane structure [57].

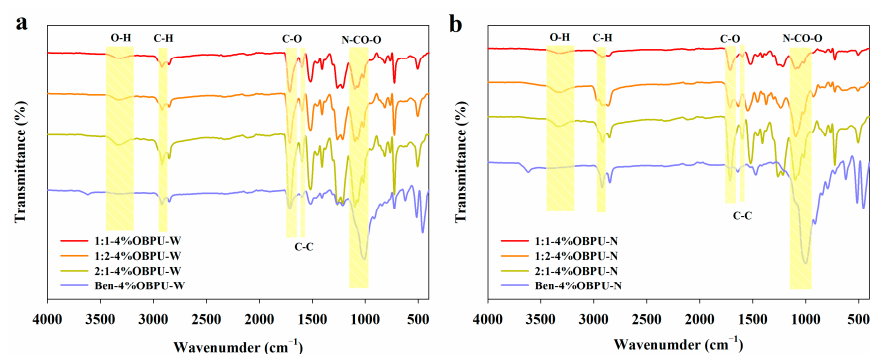


**Figure 10.** FTIR spectra of 4% soybean-oil-based polyurethanes (PGL1:1, 1:2, 2:1, HN, and Ben) in (b) and out (a) of controlled-release KCl membrane shell.

### 3.10. Scanning Electron Microscopy of Controlled-Release Potassium Chloride Fertilizers and Membrane Shells

In analyzing the fertilizer shells to which varying proportions of the PGL binder were added (as depicted in Figure 11(a1–c1)), it was observed that the shells from all three treatments exhibited differences in porosity. Specifically, the PGL2:1 treatment product displayed the least porous structure, whereas the PGL1:1 treatment predominantly showcased a porous coating. This increased porosity in the latter might be the primary reason for the elevated initial stage release rate of the fertilizer. We deduced that an overabundance of potassium ions can expedite the formation of the polyurethane gel, rendering the reaction uncontrollable. This observation was further corroborated by magnified images (Figure 11(a2,a3,b2,b3,c2,c3)), revealing a degree of porosity in the shell. Furthermore, SEM images of the cross-sections for the three treatments (Figure 11(a4,a5,b4,b5,c4,c5)) demonstrated that the coating from the PGL2:1 treatment was tightly adhered to the surface of the fertilizer core post-reaction. Conversely, the other two treatments exhibited cracks at the interface between the coating and fertilizer cores, which might account for the notable disparity in cumulative release rates. A plausible explanation for this could be the cross-linking of the polyurethane in the PGL2:1 treatment with the hydroxyl groups present on the modified lignin during the reaction. Owing to the significant proportion of modified lignin in the binder, there was enhanced adherence between the coating and the fertilizer core surface. In the remaining treatments, observable gaps and localized pores were present. This not only expedited the permeation of water molecules but also compromised the interfacial strength upon granule compression, thus facilitating rapid nutrient release.

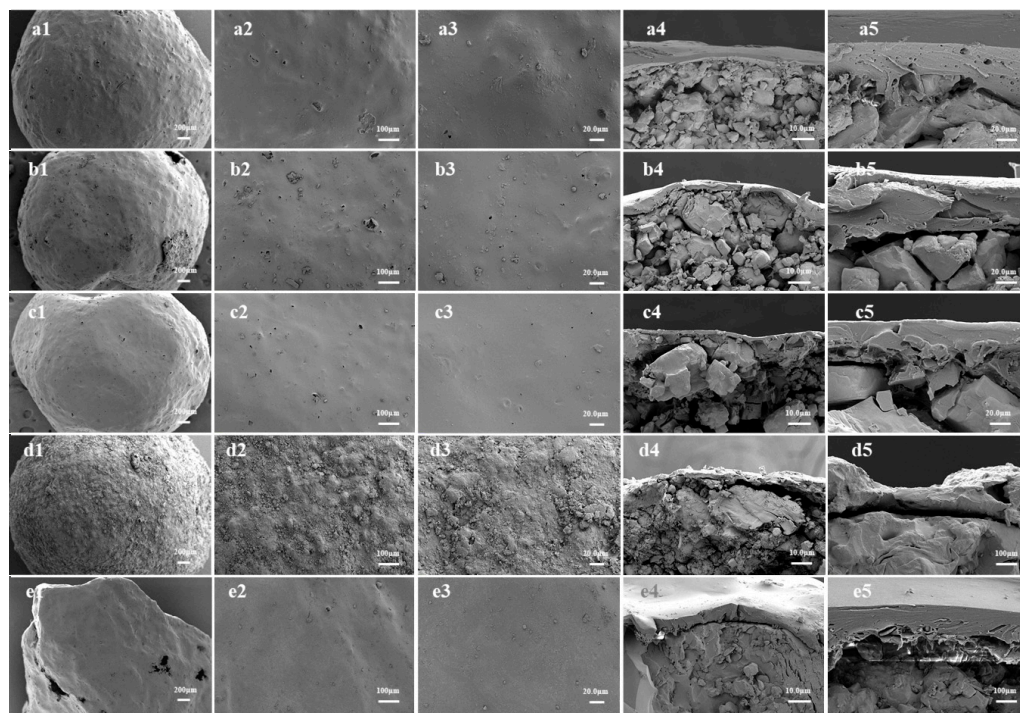


**Figure 11.** SEM images of the membrane shell and fertilizer of (a) PGL2:1-4%-OBPU, (b) PGL1:1-4%-OBPU, (c) PGL1:2-4%-OBPU, (d) Ben-4%-OBPU, and (e) HN-4%-OBPU. Panels 1 (a1–e1), 2 (a2–e2), 3 (a3–e3), the membrane surface after 50 times, 100 times, and 500 times image amplification, respectively, and panels 4 (a4–e4) and 5 (a5–e5) after 100 times and 5000 times image amplification.

For the fertilizer membrane shell with added bentonite (as illustrated in Figure 11(d1)), the surface appeared rough and displayed irregular protrusions. This texture was attributed to the excessive inclusion of bentonite in the fertilizer core, which interfered

with the polyurethane reaction, although it did not affect the fertilizer's inherent properties. When an overabundance of bentonite was present, it infiltrated the polyurethane precursor, leading to the manifestation of small pores and defects in the polymer. As a consequence, the physical properties of the resultant polymer were compromised. Enlarged images (Figure 11(d2,d3)) depicted an uneven and incomplete surface resultant from the polyurethane reaction, which was potentially due to an extended reaction time. This imperfection enhanced the contact area between water molecules and the membrane shell, facilitating the rapid permeation of water into the membrane and, thereby, expediting the dissolution and release of potassium chloride [58]. Additionally, the cross-sectional images of the bentonite-treated fertilizer (Figure 11(d4,d5)) revealed that, due to the excessive presence of bentonite, the adhesion between the membrane shell and fertilizer was not optimal. Further, observable gaps were present, contributing to the accelerated release of nutrients.

For the HN potassium chloride fertilizer (as depicted in Figure 11(e1)), significant pores were observed on the membrane shell's surface, compromising its controlled-release capability. When faced with a lower coating rate, the membrane did not achieve full coverage, leading to the emergence of cracks in the coating. Consequently, the fertilizer core came into direct contact with water, promoting rapid nutrient release. The magnified visuals (Figure 11(e2,e3)) highlighted an inconsistent coating thickness, which was attributable to the irregular surface topology. The membrane's reduced thickness in the pronounced fault sections of the fertilizer core allowed water to easily penetrate the protrusions, facilitating nutrient dissolution and expediting their transport. The cross-sectional images (Figure 11(e4,e5)) further revealed a discernible gap between the membrane shell and the fertilizer, which expedited the nutrient release process.

### 3.11. Laser Scanning of the Morphology of Potassium Chloride Fertilizer Cores

One of the most important factors affecting the rate of nutrient release from controlled-release fertilizers was the shape of the fertilizer core, and the release rate of coated fertilizer granules depended on the thinnest position of the whole coating, as shown in Figure S5 [13]. The irregular shape of the fertilizer core caused the coating overall thickness to be uneven. The nutrient release rate and time of controlled-release fertilizers were impacted by the ratio of the surface area to the fertilizer core volume [59]. In general, the nutrient release rate and time increased as the surface area of fertilizer cores increased. In a certain range of granule sizes (2–5 mm), the specific surface area of irregular granules was larger than that of regular spherical granules. At the same weight (0.0752 g), the surface area of PGL2:1 KCl granules was 68.3733 mm<sup>2</sup>, while that of HN KCl granules was 82.5051 mm<sup>2</sup>, an increase of 20.67%. The application of fertilizer cores with a high roundness and smooth surfaces reduced the amount of coating material needed and brought the membrane shell thickness close to the ideal level [60].

## 4. Conclusions

This study focused on using a modified lignin polyurea binder on agglomeration granulation to create spherical controlled-release potassium chloride fertilizer cores. According to FTIR analysis, we successfully produced high-performance polyurea via lignin modification, which raised the amino group of the lignin and improved its compatibility with polyurea. The lignin-containing polyurea binder was synthesized via a process of grafting urea onto lignin and partial polyether amine replacement. The thermal stability of polyurea binders was also enhanced via lignin addition. The 1:2 mass ratio of urea to lignin was chosen as the ideal material ratio based on the excellent application performance of the modified binder (e.g., viscosity, dry bonding strength, tensile strength, elongation at break, granule intensity, and the supplementary angle of the sliding angle). Under these conditions, fertilizer granules had good physical properties, including a hardness of 35.8 N; a resting angle and sliding angle of 15.5° and 15.3°, respectively; and a moisture absorption of 0.03%. The coating test showed that ions with a high concentration reduced the durability,

adhesion, hardness, impact resistance, and corrosion resistance of polyurethane coatings. However, due to the binder containing lignin in the fertilizer, the benzene ring and hydroxyl group in the binder reduced the extent of damage to the polyurethane membrane, which was beneficial for the normal release of coated fertilizer. The modified lignin polyurea binder has great potential for manufacturing a controlled-release potassium fertilizer. In the future, more renewable resources will be developed, such as crop straw, starch, and cellulose, to replace all petrochemical resources. Self-healing technology was introduced into fertilizer granulation to improve fertilizer properties, and fertilizer particles with a higher particle strength and better roundness were prepared.

**Supplementary Materials:** The following supporting information can be downloaded at <https://www.mdpi.com/article/10.3390/agronomy13102641/s1>. Figure S1: The flow chart of the modified polyurea binder controlled-release potassium chloride process.; Figure S2: The thermogravimetric experiment results for polyurea adhesives; Figure S3: DSC reheating curve of lignin-based polyurea binder; Figure S4: Image of grain roundness of potassium chloride fertilizer; Figure S5: HN (a) and PGL2:1 (b) potassium chloride laser scould custom view; Table S1: Synthesis formula of urea grafted lignin; Table S2: Lignin grafted rate of different lignin and urea ratios; Table S3: Synthesis formula of modified lignin polyurea; Table S4: Different binders and add ratios; Table S5: The results for the thermogravimetric test of polyurea adhesives; Table S6: Quantitative classification of radar images.

**Author Contributions:** Conceptualization, methodology, formal analysis, data curation, writing—original draft, writing—review and editing, M.L.; formal analysis, G.E., R.S. and J.W.; data curation, C.W. and S.W.; resources, Y.W.; methodology, Z.L. (Zeli Li) and Q.C.; conceptualization, investigation, funding acquisition, writing—original draft, supervision, writing—review and editing, Z.L. (Zhiguang Liu). All authors have read and agreed to the published version of the manuscript.

**Funding:** This study was supported by the Shandong Province Youth Innovation Team Project (2022KJ237).

**Data Availability Statement:** The data presented in this study are available on request from the corresponding author.

**Conflicts of Interest:** The authors declare no conflict of interest.

## References

1. Nadarajan, S.; Sukumaran, S. Chemistry and Toxicology behind Chemical Fertilizers. In *Controlled Release Fertilizers for Sustainable Agriculture*; Academic Press: Cambridge, MA, USA, 2021; pp. 195–229.
2. Al Rawashdeh, R.; Maxwell, P. Analysing the world potash industry. *Resour. Policy* **2014**, *41*, 143–151. [[CrossRef](#)]
3. Fixen, P.E.; Johnston, A.M. World fertilizer nutrient reserves: A view to the future. *J. Sci. Food Agric.* **2012**, *92*, 1001–1005. [[CrossRef](#)]
4. Al Rawashdeh, R.; Xavier-Oliveira, E.; Maxwell, P. The potash market and its future prospects. *Resour. Policy* **2016**, *47*, 154–163. [[CrossRef](#)]
5. Blanco, M. *Supply of and Access to Key Nutrients NPK for Fertilizers for Feeding the World in 2050*; UPM: Madrid, Spain, 2011.
6. Dobermann, A. Nutrient use efficiency—Measurement and management. In *Fertilizer Best Management Practices: General Principles, Strategy for Their Adoption and Voluntary Initiatives Versus Regulations*; Krauss, A., Isherwood, K., Heffer, P., Eds.; International Fertilizer Industry Association: Paris, France, 2007; pp. 1–28.
7. Al-Rawajfeh, A.E.; Alrbaihat, M.R.; AlShamaileh, E.M. Characteristics and types of slow-and controlled-release fertilizers. In *Controlled Release Fertilizers for Sustainable Agriculture*; Academic Press: Cambridge, MA, USA, 2021; pp. 57–78.
8. Vejan, P.; Khadiran, T.; Abdullah, R.; Ahmad, N. Controlled release fertilizer: A review on developments, applications and potential in agriculture. *J. Control. Release* **2021**, *339*, 321–334. [[CrossRef](#)]
9. Abbas, A.; Wang, Z.; Zhang, Y.; Zhang, Y.R.; Peng, P.; She, D. Lignin-based controlled release fertilizers: A review. *Int. J. Biol. Macromol.* **2022**, *222*, 1801–1817. [[CrossRef](#)]
10. Yang, X.Y.; Geng, J.B.; Li, C.L.; Zhang, M.; Chen, B.C.; Tian, X.F.; Zheng, W.K.; Liu, Z.G.; Wang, C. Combined application of polymer coated potassium chloride and urea improved fertilizer use efficiencies, yield and leaf photosynthesis of cotton on saline soil. *Field Crops Res.* **2016**, *197*, 63–73. [[CrossRef](#)]
11. Li, J.; Zhuang, X.G.; Font, O.; Moreno, N.; Vallejo, V.R.; Querol, X.; Tobias, A. Synthesis of merlinoite from Chinese coal fly ashes and its potential utilization as slow releases K-fertilizer. *J. Hazard. Mater.* **2014**, *265*, 242–252. [[CrossRef](#)] [[PubMed](#)]
12. Stewart, J.A. Potassium sources, use, and potential. In *Potassium in Agriculture*; Wiley: Hoboken, NJ, USA, 1985; pp. 83–98.

13. Tian, H.Y.; Zhang, L.N.; Dong, J.J.; Wu, L.; Fang, F.L.; Wang, Y.F.; Li, H.; Xie, C.S.; Li, W.J.; Wei, Z.B.; et al. A one-step surface modification technique improved the nutrient release characteristics of controlled-release fertilizers and reduced the use of coating materials. *J. Clean. Prod.* **2022**, *369*, 133331. [[CrossRef](#)]
14. Guo, Y.L.; Liu, Z.G.; Zhang, M.; Tian, X.F.; Chen, J.Q.; Sun, L.L. Synthesis and application of urea-formaldehyde for manufacturing a controlled-release potassium fertilizer. *Ind. Eng. Chem. Res.* **2018**, *57*, 1593–1606. [[CrossRef](#)]
15. Loganathan, P.; Hedley, M.J.; Clark, S.A. The manufacture and evaluation of granular potassium chloride fertilizers. *Fert. Res.* **1992**, *31*, 291–304. [[CrossRef](#)]
16. Prasai, T.P.; Walsh, K.B.; Midmore, D.J.; Jones, B.E.H.; Bhattarai, S.P. Manure from biochar, bentonite and zeolite feed supplemented poultry: Moisture retention and granulation properties. *J. Environ. Manag.* **2018**, *216*, 82–88. [[CrossRef](#)] [[PubMed](#)]
17. Washino, K.; Tan, H.S.; Hounslow, M.J.; Salman, A.D. A new capillary force model implemented in micro-scale CFD–DEM coupling for wet granulation. *Chem. Eng. Sci.* **2013**, *93*, 197–205. [[CrossRef](#)]
18. Albadarin, A.B.; Lewis, T.D.; Walker, G.M. Granulated polyhalite fertilizer caking propensity. *Powder Technol.* **2017**, *308*, 193–199. [[CrossRef](#)]
19. Jacob, M. Spheronization, granulation, pelletization, and agglomeration processes. In *Microencapsulation in the Food Industry*; Academic Press: Vienna, Austria, 2023; pp. 123–136.
20. Degève, J.; Baeyens, J.; Van de Velden, M.; Laet, S.D. Spray-agglomeration of NPK-fertilizer in a rotating drum granulator. *Powder Technol.* **2006**, *163*, 188–195. [[CrossRef](#)]
21. Mathur, M.A.; Dias, M.F.; Mathur, M.P. Importance of green technology in fertilizer quality improvement. *Procedia Eng.* **2016**, *138*, 308–313. [[CrossRef](#)]
22. Subero-Couroyer, C.; Ghadiri, M.; Brunard, N.; Kolenda, F. Analysis of catalyst particle strength by impact testing: The effect of manufacturing process parameters on the particle strength. *Powder Technol.* **2005**, *160*, 67–80. [[CrossRef](#)]
23. Kabiri, S.; Baird, R.; Tran, D.N.H.; Andelkovic, I.; McLaughlin, M.J.; Losic, D. Cogranulation of low rates of graphene and graphene oxide with macronutrient fertilizers remarkably improves their physical properties. *ACS Sustain. Chem. Eng.* **2018**, *6*, 1299–1309. [[CrossRef](#)]
24. Secco, M.; Valentini, L.; Addis, A. Ancient and modern binders: Naturally nanostructured materials. In *Nanotechnologies and Nanomaterials for Diagnostic. Conservation and Restoration of Cultural Heritage*; Elsevier: Amsterdam, The Netherlands, 2019; pp. 205–237.
25. Zhang, G.J.; Sun, Y.H.; Xu, Y. Review of briquette binders and briquetting mechanism. *Renew. Sustain. Energy Rev.* **2018**, *82*, 477–487. [[CrossRef](#)]
26. Xue, B.C.; Liu, T.; Huang, H.; Liu, E.B. The effect of the intimate structure of the solid binder on material viscosity during drum granulation. *Powder Technol.* **2014**, *253*, 584–589. [[CrossRef](#)]
27. De La Grée, G.C.H.D.; Florea, M.V.A.; Keulen, A.; Brouwers, H.J.H. Contaminated biomass fly ashes—Characterization and treatment optimization for reuse as building materials. *Waste Manag.* **2016**, *49*, 96–109. [[CrossRef](#)] [[PubMed](#)]
28. Skeist, I.; Miron, J. History of adhesives. *J. Macromol. Sci. Chem.* **1981**, *15*, 1151–1163. [[CrossRef](#)]
29. Liu, K.K.; Su, C.Q.; Ma, W.W.; Li, H.L.; Zeng, Z.; Li, L.Q. Free formaldehyde reduction in urea-formaldehyde resin adhesive: Modifier addition effect and physicochemical property characterization. *BioResources* **2020**, *15*, 2339–2355. [[CrossRef](#)]
30. Conner, A.H. Urea-formaldehyde adhesive resins. In *Polymeric Materials Encyclopedia*; Salamone, J.C., Ed.; CRC Press: New York, NY, USA, 1996; Volume 11.
31. Balčiūnas, G.; Vėjelis, S.; Vaitkus, S.; Kairytė, A. Physical properties and structure of composite made by using hemp hurds and different binding materials. *Procedia Eng.* **2013**, *57*, 159–166. [[CrossRef](#)]
32. Gironès, J.; López, J.P.; Mutjé, P.; Curvelo, A.A.S.; Vilaseca, F. Natural fiber-reinforced thermoplastic starch composites obtained by melt processing. *Compos. Sci. Technol.* **2012**, *72*, 858–863. [[CrossRef](#)]
33. Kremensas, A.; Kairytė, A.; Vaitkus, S.; Vėjelis, S. Physical-mechanical properties of Composites from Hemp Shives and Starch. *Int. J. Eng. Sci. Invent.* **2018**, *7*, 43–49.
34. Shim, J.; Mohr, D. Using split Hopkinson pressure bars to perform large strain compression tests on polyurea at low, intermediate and high strain rates. *Int. J. Impact Eng.* **2009**, *36*, 1116–1127. [[CrossRef](#)]
35. Liu, W.; Fang, C.; Chen, F.T.; Qiu, X.Q. Strong, reusable, and self-healing lignin-containing polyurea adhesives. *ChemSusChem* **2020**, *13*, 4691–4701. [[CrossRef](#)]
36. Li, T.; Xie, Z.N.; Xu, J.; Weng, Y.X.; Guo, B.H. Design of a self-healing cross-linked polyurea with dynamic cross-links based on disulfide bonds and hydrogen bonding. *Eur. Polym. J.* **2018**, *107*, 249–257. [[CrossRef](#)]
37. Li, T.H.; Zhang, B.G.; Jiang, S.Y.; Zhou, X.J.; Du, G.B.; Wu, Z.G.; Cao, M.; Yang, L. Novel highly branched polymer wood adhesive resin. *ACS Sustain. Chem. Eng.* **2020**, *8*, 5209–5216. [[CrossRef](#)]
38. Shojaei, B.; Najafi, M.; Yazdanbakhsh, A.; Abtahi, M.; Zhang, C.W. A review on the applications of polyurea in the construction industry. *Polym. Adv. Technol.* **2021**, *32*, 2797–2812. [[CrossRef](#)]
39. Luo, J.Z.; Wang, T.; Sim, C.; Li, Y.Z. Mini-Review of Self-Healing Mechanism and Formulation Optimization of Polyurea Coating. *Polymers* **2022**, *14*, 2808. [[CrossRef](#)]
40. Wu, H.Z.; Liao, D.S.; Chen, X.Y.; Du, G.B.; Li, T.H.; Essawy, H.; Pizzi, A.; Zhou, X.J. Functionalized Natural Tannins for Preparation of a novel non-isocyanate polyurea-based adhesive. *Polym. Test.* **2023**, *117*, 107853. [[CrossRef](#)]

41. Klapiszewski, L.; Szalaty, T.; Jesionowski, T. Lignin as Material of the Future: Key Information and Development Prospects. *Encycl. Polym. Sci. Technol.* **2002**, 1–28. [[CrossRef](#)]
42. Zhao, X.H.; Zhang, Y.J.; Hu, H.Y.; Huang, Z.Q.; Qin, Y.B.; Shen, F.; Huang, A.M.; Feng, Z.F. Effect of lignin esters on improving the thermal properties of poly (vinyl chloride). *J. Appl. Polym. Sci.* **2019**, *136*, 47176. [[CrossRef](#)]
43. Yang, G.T.; Zhao, H.M.; Liu, Y.L.; Li, Z.L.; Gao, F.; Zhang, Q.; Zou, P.; Liu, Z.G.; Zhang, M. Slow release fertilizers based on polyphosphate/montmorillonite nanocomposites for improving crop yield. *Arab. J. Chem.* **2023**, *16*, 104871. [[CrossRef](#)]
44. Tian, H.Y.; Liu, Z.G.; Zhang, M.; Guo, Y.L.; Zheng, L.; Li, Y.C.C. Biobased polyurethane, epoxy resin, and polyolefin wax composite coating for controlled-release fertilizer. *ACS Appl. Mater. Interfaces* **2019**, *11*, 5380–5392. [[CrossRef](#)]
45. Dubey, A.; Mailapalli, D.R. Zeolite coated urea fertilizer using different binders: Fabrication, material properties and nitrogen release studies. *Environ. Technol. Innov.* **2019**, *16*, 100452. [[CrossRef](#)]
46. Ferreira, I.S.B.; Peruchi, R.S.; Fernandes, N.J.; Junior, P.R. Measurement system analysis in angle of repose of fertilizers with distinct granulometries. *Measurement* **2021**, *170*, 108681. [[CrossRef](#)]
47. Fang, C.; Liu, W.F.; Qiu, X.Q. Preparation of polyetheramine-grafted lignin and its application in UV-resistant polyurea coatings. *Macromol. Mater. Eng.* **2019**, *304*, 1900257. [[CrossRef](#)]
48. Wang, S.Y.; Liu, W.F.; Yang, D.J.; Qiu, X.Q. Highly resilient lignin-containing polyurethane foam. *Ind. Eng. Chem. Res.* **2018**, *58*, 496–504. [[CrossRef](#)]
49. Dhenge, R.M.; Washino, K.; Cartwright, J.J.; Hounslow, M.J.; Salman, A.D. Twin screw granulation using conveying screws: Effects of viscosity of granulation liquids and flow of powders. *Powder Technol.* **2013**, *238*, 77–90. [[CrossRef](#)]
50. Lapprand, A.; Boisson, F.; Delolme, F.; Méchin, F.; Pascault, J.P. Reactivity of isocyanates with urethanes: Conditions for allophanate formation. *Polym. Degrad. Stab.* **2005**, *90*, 363–373. [[CrossRef](#)]
51. Dušek, K. Theory of network formation by additional crosslinking of polyurethanes due to biuret and allophanate formation. *Polym. Bull.* **1987**, *17*, 481–488. [[CrossRef](#)]
52. Xu, Q.W.; Lu, Q.L.; Zhu, S.; Pang, R.; Shan, W.W. Effect of resins on the salt spray resistance and wet adhesion of two component waterborne polyurethane coating. *e-Polymers* **2019**, *19*, 444–452. [[CrossRef](#)]
53. Joulazadeh, M.; Navarchian, A.H. Effect of process variables on mechanical properties of polyurethane/clay nanocomposites. *Polym. Adv. Technol.* **2010**, *21*, 263–271. [[CrossRef](#)]
54. Chen, B.; Peng, F.; Zhang, L.; Sun, D.A. Investigation on swelling characteristics of GMZ bentonite with different initial water contents. *Ann. Nucl. Energy* **2023**, *181*, 109565. [[CrossRef](#)]
55. Chio, C.L.; Sain, M.; Qin, W.S. Lignin utilization: A review of lignin depolymerization from various aspects. *Renew. Sustain. Energy Rev.* **2019**, *107*, 232–249. [[CrossRef](#)]
56. Sensui, K.; Tarui, T.; Miyamae, T.; Sato, C. Evidence of chemical-bond formation at the interface between an epoxy polymer and an isocyanate primer. *Chem. Commun.* **2019**, *55*, 14833–14836. [[CrossRef](#)]
57. Lu, P.F.; Zhang, Y.F.; Jia, C.; Li, Y.F.; Zhang, M.; Mao, Z.Q. Degradation of polyurethane coating materials from liquefied wheat straw for controlled release fertilizers. *J. Appl. Polym. Sci.* **2016**, *133*, 25. [[CrossRef](#)]
58. Zhang, S.G.; Yang, Y.C.; Gao, B.; Wan, Y.S.; Li, Y.C.C.; Zhao, C.H. Bio-based interpenetrating network polymer composites from locust sawdust as coating material for environmentally friendly controlled-release urea fertilizers. *J. Agric. Food Chem.* **2016**, *64*, 5692–5700. [[CrossRef](#)] [[PubMed](#)]
59. Liu, L.; Shen, T.L.; Yang, Y.C.; Gao, B.; Li, Y.C.C.; Xie, J.Z.; Tang, Y.F.; Zhang, S.G.; Wang, Z.H.; Chen, J.Q. Bio-based large tablet controlled-release urea: Synthesis, characterization, and controlled-released mechanisms. *J. Agric. Food Chem.* **2018**, *66*, 11265–11272. [[CrossRef](#)] [[PubMed](#)]
60. Lu, H.; Tian, H.Y.; Liu, Z.G.; Zhang, M.; Zhao, C.H.; Guo, Y.L.; Guan, R.; Chen, Q.; Yu, X.J.; Wang, H.L.; et al. Polyolefin wax modification improved characteristics of nutrient release from biopolymer-coated phosphorus fertilizers. *ACS Omega* **2019**, *4*, 20402–20409. [[CrossRef](#)] [[PubMed](#)]

**Disclaimer/Publisher’s Note:** The statements, opinions and data contained in all publications are solely those of the individual author(s) and contributor(s) and not of MDPI and/or the editor(s). MDPI and/or the editor(s) disclaim responsibility for any injury to people or property resulting from any ideas, methods, instructions or products referred to in the content.